CYLINDER DECOMPOSITIONS ON GEOMETRIC ARMADILLO TAILS

DAMI LEE AND JOSH SOUTHERLAND

ABSTRACT. We study a particular type of finite area, infinite-type translation surfaces, and find explicit examples of types of cylinder decompositions on these surfaces which do not manifest on finite-type translation surfaces.

1. INTRODUCTION AND DEFINITIONS

A translation surface is a (countable) collection of polygons in the plane where all sides are paired with a side of equal length such that inward pointing normal vectors for each side point in opposite directions after identification. Finite translation surfaces are collections of finitely many polygons with only finitely many sides, whereas infinite translation surfaces allow for constructions containing countably many polygons or infinitely many sides on a single polygon. See, for example, [4].

In this article, we will simply refer to infinite-type translations surfaces as translation surfaces. We define a particular translation surface to study, which we call an *armadillo tail surface*, or *armadillo tail*. We place a square, which we denote by $\square_1$, in the first quadrant so that the lower left vertex lies at the origin and all edges are parallel to the axes. For $k \geq 1$, glue the left side of $\square_{k+1}$ to the right side of $\square_k$ so that the bottom edge of all squares lie on the x-axis. We denote the side length of $\square_n$ by l_n, and assume that (l_n) is a strictly decreasing sequence. We then identify horizontal (vertical, resp.) edges via vertical (horizontal, resp.) translation. Bowman [2] and Degli Esposti–Del Magno–Lenci [3] have also built infinite-type translation surfaces in a similar fashion but allowed rectangles instead of squares; the surface in the former article is known as a "stack of boxes" and the one in the latter, "Italian billiards."

The following are examples of finite-area armadillo tail surfaces.

Example 1.1. (1) The armadillo tail surface where $l_n = r^{n-1}$, for $r \in (0,1)$, which we call a *geometric armadillo* with parameter r. Its area is $\frac{1}{1-r^2}$.

(2) The *harmonic armadillo tail* where $l_n = \frac{1}{n}$. While the surface is not bounded in the horizontal direction, its area is finite and $\zeta(2) = \frac{\pi^2}{6}$.

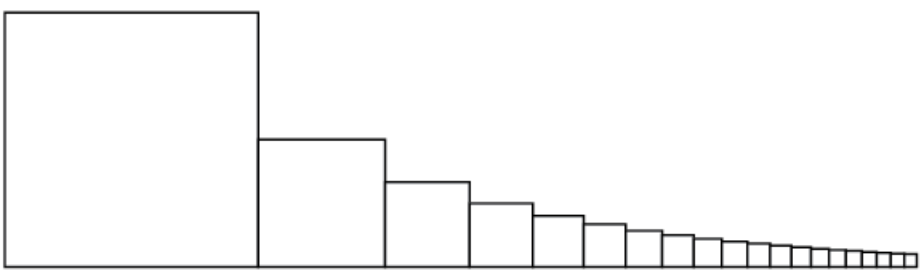

FIGURE 1. The harmonic armadillo tail surface

We attain a finite translation surface we call the *truncated armadillo tail* which is $\bigcup_{i=1}^{n} \square_i$ where we make the same identifications as above, except that we identify the right edge of $\square_n$ with the bottom segment of the left edge of $\square_1$. We denote the truncated armadillo tail by X_n.

Without loss of generality, we assume that $l_1 = 1$. With horizontal (vertical, resp.) edges being identified via vertical (horizontal, resp.) translation, the resulting translation surface is an infinite genus surface (infinite connected sum of square tori) with one (wild) singularity. For background on wild singularities, see [2], [4], [8]. The wild singularity appears infinitely many times in the polygonal representation of the surface: each vertex of the infinite-sided polygon is the same point on the surface. We note that Bowman's "stack of boxes" also has one wild singularity, but the "Italian billiards" of Degli Esposti-Del Magno-Lenci have many cone points, none of which are wild.

We consider armadillo tails concrete, toy examples that can be used for prodding at both the geometric and dynamical properties of finite area, infinite-type translation surfaces with one wild singularity (and no other singularities). In what follows, our focus is on a purely geometric construction: a cylinder decomposition on this surface. Finding cylinder decompositions on a surface is challenging, even on finite translation surfaces. Here, we are able to leverage the structure of the surface to inductively construct cylinders.

We begin with definitions, and an example, before stating the main result. A *cylinder* is a closed subspace of the surface whose interior is foliated by homotopic closed straight-line trajectories, and whose boundary consists of saddle connections, line segments whose endpoints coincide with a singular point. A closed trajectory in a cylinder is called a *waist curve*. The *circumference* of a cylinder is the length of a closed straight-line trajectory, and the *width* of a cylinder is the distance between the bounding saddle connections. A *cylinder decomposition* is the closure of a union of possibly infinitely many cylinders whose waist curves are in the same direction and which covers the surface. Further, we require that each cylinder in the cylinder decomposition only intersect another cylinder at most along a saddle connection. The closure of the union of cylinders may contain a line segment that is not in any cylinder which we call a *spine*. A spine may be a concatenation of possibly infinitely many saddle connections. If a spine is made of a single saddle connection, we call it a *rigid spine.* If a spine is comprised of multiple (possibly infinitely many) saddle connections, we call it a *flexible spine*.

As an example, consider the cylinder decomposition $\mathcal{C}$ of an armadillo tail in the rather obvious horizontal direction, given our choice of polygonal representation of the surface. See Figure 2.

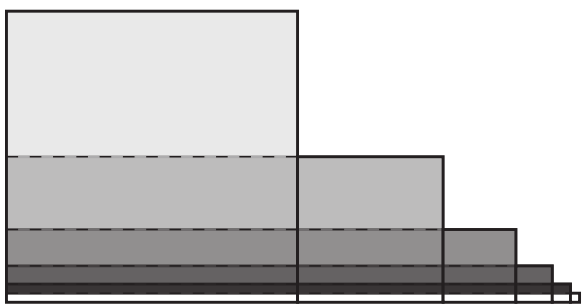

FIGURE 2. A cylinder decomposition of a geometric armadillo tail in the horizontal direction

Observe that as we move from top to bottom, each cylinder in the cylinder decomposition becomes longer and thinner, eventually limiting to a flexible spine at the base of the polygonal representation (the closed trajectory comprised of an infinite concatenation of saddle connections).

There is another cylinder decomposition intimately related to the above cylinder decomposition, what we call the *orthogonal cylinder decomposition*, $\mathcal{C}^\perp$. In the original cylinder decomposition shown in Figure 2, label the cylinders numerically from top to bottom, cyl_k. Then, $\text{cyl}_1^\perp$, the first cylinder in $\mathcal{C}^\perp$ has width equal to the circumference of cyl_1 in $\mathcal{C}$. The circumference of $\text{cyl}_1^\perp$ is equal to the sum of all of the widths of the cylinders in the original cylinder decomposition. Similarly, the $\text{cyl}_2^\perp$ has width equal to the height cyl_2 less the height of the cyl_1. The circumference of $\text{cyl}_2^\perp$ is the sum of all of the widths of the cylinders in $\mathcal{C}$ less the width of cyl_1. Each subsequent cylinder is defined in the same manner. See Figure 3.

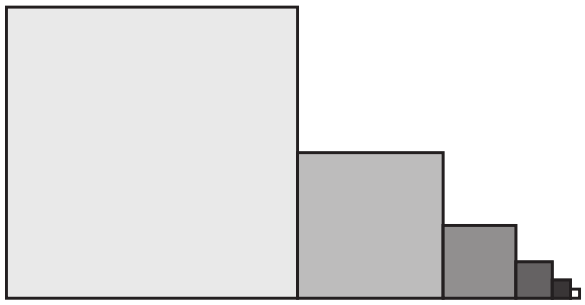

FIGURE 3. A cylinder decomposition of a armadillo tail in the vertical direction

Remark 1.2. Observe that the modulus of each cylinder in the orthogonal cylinder decomposition is 1. This implies that there exists an affine diffeomorphism of the surface ϕ such that $D\phi = \begin{bmatrix} 1 & 0 \\ 1 & 1 \end{bmatrix}$, where $D\phi$ is an element in the Veech group. See Appendix D in [5] for additional information. Observe that $D\phi$ is a parabolic element in $SL_2(\mathbb{R})$. We will refer to an affine diffeomorphism whose derivative is a parabolic element as a *parabolic affine diffeomorphism*.

1.1. **Main results.** There is another less obvious cylinder decomposition on the surface which does not appear in the orbit of this horizontal cylinder decomposition (orbit of the group of affine automorphisms of the surface). In the same way that the above cylinder decomposition is comprised of an infinite number of cylinders limiting to a spine, this cylinder decomposition will also. However, the distinction is that this one limits to a rigid spine, not a flexible spine.

Theorem 1.3. There exists a cylinder decomposition with a rigid spine on any geometric armadillo tail of parameter $\frac{1}{q}$, $q \in \mathbb{N} \setminus \{1\}$. Moreover, there is no parabolic affine diffeomorphism of the surface that fixes this cylinder decomposition.

The proof of the theorem is constructive. In Section 2, we identify a core curve - turns out to be the rigid spine. This curve wraps around every torus in the surface. Then we construct two cylinders, which become the base case in an induction proof. In Section 3, we inductively construct a set of saddle connections which turn out to be the "bottom" boundary saddle connections on each cylinder. Then we construct the cylinder decomposition by leveraging the structure of the surface. We define a (discontinuous) map which pushes a cylinder to a subset of the next widest

cylinder in the decomposition. We call the subset of a cylinder a "partial cylinder." See Section 3 for a definition. We "fill in" the missing segments of the cylinder using a circle rotation argument. Indeed, the endpoints of the partial cylinder correspond to periodic points of a circle rotation. In Section 4, we compute the modulus and area of each cylinder in the cylinder decomposition.

It seems feasible to extend our methods to the case of $r = \frac{p}{q}$, provided one can find enough cylinders to start the induction process. Moreover, the induction process may involve fixed points of a finite-type interval exchange transformation (IET) in lieu of a circle rotation. See [10] for a description of IETs.

In Section 5, we show that there cannot be a parabolic element that stabilizes the cylinder decomposition that we construct. Moreover, we note that the orthogonal cylinder decomposition to this cylinder decomposition *does not exist*.

1.2. **Related work.** Bowman studies the "geometric limit" of finite-type translation surfaces converging to an infinite-type translation surface [1]. Along these lines, we can think of a geometric armadillo tail as the limit of a sequence of finite-type translation surfaces. Indeed, consider the truncated surface X_n. The cylinder in the direction of slope $\frac{1}{2-r}$ persists for all surfaces in this sequence. Moreover, for all finite-type surfaces in the sequence, there is a parabolic element that preserves both this cylinder decomposition and another that preserves the orthogonal cylinder decomposition. However, in the limit, the cylinders converge to a cylinder decomposition, but the parabolic affine diffeomorphism does not converge to any sensible affine map on the surface.

For particular directions on an armadillo tail, one can use Treviño's work, Theorem 3 in [9], to see if one can conclude that the linear flow in that direction is ergodic. However, there does not appear to be a (Veech) dichotomy in which each direction is either periodic or ergodic: the Veech group appears to be $\mathbb{Z}$ and not a lattice. It is an interesting question as to what ergodic measures are supported on an armadillo tail (geometric or otherwise). A generalization of a Veech dichotomy of this flavor was done for ladder surfaces by Hooper, Hubert, and Weiss [6].

Lastly, there is an open question regarding whether or not there exists an infinite-type translation surface with a Veech group that is a lattice in $SL_2(\mathbb{R})$ (see [4]). One might think that a particular geometric armadillo tail is a candidate, but it seems as though the Veech group may be $\mathbb{Z}$. A proof that the Veech group is $\mathbb{Z}$ would be interesting.

1.3. **Acknowledgements.** The authors would like to thank David Aulicino, Matt Bainbridge, and Pat Hooper for helpful conversations.

2. A PARTICULAR DIRECTION ON GEOMETRIC ARMADILLO TAILS

The following is a key theorem in which we identify a long closed saddle connection which turns out to be a (limiting) rigid spine of a cylinder decomposition on a certain family of armadillo tails. Every armadillo tail is an infinite connected sum of tori; this particular saddle connection wraps around each torus. Note that the following theorem is very general and requires no assumption on the parameter r. By $\frac{1}{2-r}$-direction, we mean the direction with slope $\frac{1}{2-r}$ relative to our polygonal representation.

Theorem 2.1. On geometric armadillo tails for any $r \in (0, 1)$, there exists a closed saddle connection in the $\frac{1}{2-r}$-direction that intersects every torus.

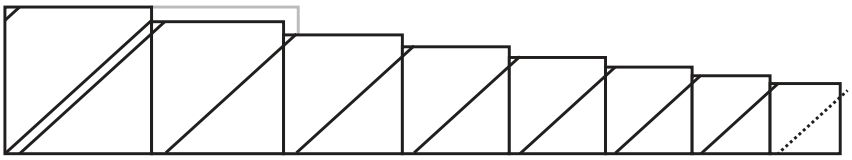

FIGURE 4. A geometric armadillo tail ($r = 9/10$) with a trajectory of slope $\frac{1}{2-r}$

Proof. We refer to the top (horizontal) edge of a square by the *roof* and the right (vertical) edge of a square that is identified to a segment on the y-axis by the *portal*.

We start from the origin, the lower left vertex of $\square_1$. Since $r < \frac{1}{2-r} < 1$, the straight line of slope $\frac{1}{2-r}$ through the origin hits the portal of $\square_1$ at point $(1, \frac{1}{2-r})$. By identification with the y-axis (the left edge of $\square_1$), the trajectory continues and hits the roof of $\square_1$ at $(1-r, 1)$. By identification with the bottom edge of $\square_1$, the trajectory continues from $(1-r, 0)$ and hits the roof of $\square_2$ at $(1 + r(1-r), r)$. The trajectory partitions both roofs with a fixed ratio. Hence, due to similarity, it hits every roof without hitting any vertex. In other words, it "wraps around every torus." □

Via renormalization (under the action of $\begin{pmatrix} 1 & 0 \\ -1 & 1 \end{pmatrix}$), one can consider the trajectory with slope $\frac{1}{2-r} - 1 = \frac{r-1}{2-r}$ direction. Starting from the upper left vertex at $(0, 1)$, the trajectory hits the portal on $\square_1$ at $\left(1, \frac{1}{2-r}\right)$. By identification, continuing from $\left(0, \frac{1}{2-r}\right)$, the trajectory does not hit any roof or portal and tends to $\left(\frac{1}{1-r}, 0\right)$, hence producing a saddle connection. In fact, given our polygonal representation, any trajectory starting from $(0, 0)$ with slope $\frac{1}{2-r} + \mathbf{n}$, for any $\mathbf{n} \in \mathbb{N}$, (or $(0, 1)$ with slope $\frac{1}{2-r} - \mathbf{n}$, for $\mathbf{n} \in \mathbb{N}$) yields a saddle connection that goes through every torus. We will see that this saddle connection is the rigid spine of a cylinder decomposition.

Moreover, the saddle connection of Theorem 2.1 has an interesting topological feature.

Proposition 2.2. The saddle connection of Theorem 2.1 is a non-separating simple closed curve.

Proof. If we color the surface on one side of the saddle connection, we will color the entire surface. □

In the following theorem, we show that for a specific family of geometric armadillo tails, i.e., when $r = \frac{1}{q}$ for $q \in \mathbb{N} \setminus \{1\}$, there exists not only a saddle connection but a cylinder in the $\frac{1}{2-r}$-direction. We call this cylinder cyl_1, and the existence of this cylinder will be part of the base case for the induction that follows.

Theorem 2.3. Given any geometric armadillo tail with parameter $r = \frac{1}{q}$, there exists a cylinder in the $\frac{1}{2-r}$-direction, which lies entirely in $\square_1 \cup \square_2$.

There are three parts to this proof. First, we show that there is a saddle connection (in the $\frac{1}{2-r}$-direction) that lies entirely in X_2. Secondly, we will show that there is another saddle connection that lies a fixed distance above the first saddle connection. In the third step, we will show that there is no saddle connection in between the two saddle connections we construct in the previous two steps, hence yielding a cylinder.

Definition 2.4. We define the *skew width of* cyl_1 as the vertical distance (vertical in relation to the polygonal representation) between the two boundary saddle connections of cyl_1 through the cylinder. Assuming cyl_k exists, we define the skew width of cyl_k similarly.

Proof. Note, for $q = \mathbb{N} \setminus \{1\}$, the slope of the trajectory is $\frac{1}{2-r} = \frac{q}{2q-1}$.

Step 1. We show that the trajectory from $(1,0)$ with slope $\frac{q}{2q-1}$ stays entirely in X_2.

Start from $(1,0)$ we hit the portal of $\square_2$ at $\left(1+\frac{1}{q}, \frac{1}{2q-1}\right)$, hence the first point at which the trajectory hits the vertical axis is at $\left(0, \frac{1}{2q-1}\right)$. We continue and hit $\left(1, \frac{1+q}{2q-1}\right)$, and since $\frac{1}{q} < \frac{1+q}{2q-1} < 1$, the trajectory goes through the portal and is identified to $\left(0, \frac{1+q}{2q-1}\right)$. Note that if we keep hitting the portal, the nth time the trajectory hits the vertical axis is at $\left(0, \frac{1}{2q-1} + \frac{(n-1)q}{2q-1} - \lfloor \frac{1}{2q-1} + \frac{(n-1)q}{2q-1} \rfloor\right)$. In fact, since $\frac{1}{2q-1} < \frac{1}{q} < \frac{2}{2q-1}$, which means that we will always hit the portal, unless the numerator of $\frac{1}{2q-1} + \frac{(n-1)q}{2q-1} - \lfloor \frac{1}{2q-1} + \frac{(n-1)q}{2q-1} \rfloor$ is 1. Pick $n = 2q-2$, then the trajectory hits the singularity at $(1,1)$. In other words, the trajectory goes through $\square_2$ exactly once at the beginning and stays in $\square_1$ until it hits a singularity.

Furthermore, this is the first time the trajectory hits the singularity. This follows from the fact that $\gcd(q, 2q-1) = 1$. The trajectory hits the y-axis at points $\left\{(0,y) : y \in \left\{\frac{(n-1)q+1}{2q-1} - \lfloor \frac{(n-1)q+1}{2q-1} \rfloor\right\}\right\}$. Note that the numerator of the y-coordinates in this set is

$$\{1, 1+q, 1+2q, \ldots, 1+(2q-3)q \equiv 0 \mod (2q-1)\}.$$

Note that if we had continued to add $\frac{q}{2q-1}$, we would have hit $\frac{1+(2q-2)q}{2q-1} \equiv \frac{q}{2q-1}$ and $\frac{1+(2q-1)q}{2q-1} \equiv \frac{1}{2q-1}$, which brings us back to the beginning of the sequence. In other words, the trajectory wraps around $\square_1$ exactly $2q-3$ times hitting the y-axis at $\left\{\left(0, \frac{i}{2q-1}\right)\right\}_{i=1,\neq q}^{2q-2}$.

Step 2. The saddle connection that we constructed above will serve as the "bottom" boundary saddle connection of cyl_1. Next, we will construct a saddle connection which will end up being the "top" boundary saddle connection. To do this, we will take the bottom saddle connections and show that if we shift the saddle connection vertically (in the polygonal representation) by $\frac{q-1}{q(2q-1)}$, that we find another saddle connection. In step 3 which follows, we will show that $\frac{q-1}{q(2q-1)}$ is the skew width of this cylinder.

Take the set of points where the bottom saddle connection hits the y-axis and add $\frac{q-1}{q(2q-1)}$:

$$\left\{\frac{i}{2q-1}\right\}_{i=1,\neq q}^{2q-2} + \frac{q-1}{q(2q-1)},$$

where a set + number denotes adding the number to each element of the set. We have $\left\{\frac{(i+1)q-1}{q(2q-1)}\right\}_{i=1,\neq q}^{2q-2}$ which we split into three cases: (1) $i = 1, \ldots, q-2$, (2) $i = q-1$, and (3) $i = q+1, \ldots, 2q-2$. We show that T maps (1) to (3), maps (3) into the union of (1) and (2), and maps (2) into a singularity.

Take points in (1), $(i = 1, \ldots, q-2)$, then we have

$$T\left(\frac{(i+1)q-1}{q(2q-1)}\right) = \frac{(i+1+q)q-1}{q(2q-1)} \in \left\{\frac{(i+1)q-1}{q(2q-1)}\right\}_{i=q+1}^{2q-1}.$$

Next, we take points in (3), $(i = q+1, \ldots, 2q-2)$, then for all points except $i = 2q-2$ we have

$$T\left(\frac{(i+1)q-1}{q(2q-1)}\right) = \frac{(i+1+q)q-1}{q(2q-1)} \equiv \frac{(i-q+2)q-1}{q(2q-1)} \in \left\{\frac{(i+1)q-1}{q(2q-1)}\right\}_{i=1}^{q-2}.$$

For $i = 2q-2$, we have $T\left(\frac{(2q-1)q-1}{q(2q-1)}\right) = \frac{q^2-1}{q(2q-1)} \in \left\{\frac{(i+1)q-1}{q(2q-1)}\right\}_{i=q-1}$. Lastly, for case (2), where $i = q-1$, we have

$$T\left(\frac{q^2-1}{q(2q-1)}\right) = \frac{2q^2-1}{q(2q-1)} \equiv \frac{q-1}{q(2q-1)} < \frac{1}{q}.$$

Since the trajectory hits the right side of $\square_1$ below the portal, we continue in $\square_2$ and hit $\left(1+\frac{1}{q}, \frac{1}{q}\right)$ which is a singularity. In other words, we have a second closed saddle connection through $\left(0, \frac{1}{q}\right)$ that lies entirely in $\square_1$ and $\square_2$.

Step 3. Lastly, we show that there are no saddle connections that hit the vertical axis between $\left(0, \frac{1}{2q-1}\right)$ and $\left(0, \frac{1}{q}\right)$. Since there is only one singularity $\left(0, \frac{1}{q}\right)$ in $\{0\} \times (0,1)$, we simply need the fact that there is no integer i that satisfies $\frac{i}{2q-1} < \frac{1}{q} < \frac{i}{2q-1} + \frac{q-1}{q(2q-1)}$. In the inequality, the lower bound comes from the saddle connection constructed in Step 1, and the upper bound comes from the saddle connection constructed in Step 2.

In conclusion, on a geometric armadillo tail with parameter $r = \frac{1}{q}$, there exists a cylinder that lies entirely in $\square_1$ and $\square_2$. We call this cylinder cyl_1. □

Remark 2.5. The assumption that $r = \frac{1}{q}$ cannot be removed. For example, if $r = 2/3$, the saddle connection starting from $(1,0)$ is not contained only in $\square_1$ and $\square_2$. It also passes through $\square_3$.

3. Finding successive cylinders in the $\frac{1}{2-r}$-direction

In this section, we use induction to construct the bottom saddle connection of the kth cylinder and hence the cylinder themselves in the $\frac{1}{2-r}$-direction.

We define a map f_r to construct new cylinders from existing cylinders.

Definition 3.1. The map $\tilde{f_r} : \mathbb{R}^2 \to \mathbb{R}^2$, where

$$\tilde{f_r} : \begin{pmatrix} x \\ y \end{pmatrix} \mapsto \begin{pmatrix} rx+1 \\ ry \end{pmatrix}.$$

Observe that $\tilde{f_r}$ is an injective map.

The map does not descend from $\mathbb{R}^2$ to a well-defined map on the quotient of the polygonal representation of an armadillo tail. The issue is that the map does not respect the vertical gluings (by horizontal translations). For instance, the leftmost edge of $\square_1$ is mapped to the leftmost edge of $\square_2$, but the leftmost edge of $\square_2$ is glued to the right side of $\square_2$. However, the map does descend to a partial quotient, where we only identify the top and bottom edges, since $\tilde{f_r}$ respects the identifications along the tops and bottoms of the squares. That is the content of the following lemma, whose proof is elementary.

Lemma 3.2. Let P_r be the polygonal representation of an armadillo tail X with parameter r such that the polygonal representation is embedded in $\mathbb{R}^2$ and the side identifications forgotten. Let X^{tb} be a quotient of P_r by identifying the top and bottom edges only. Let $\square_k^{tb}$ denote the k^{th}-square in X^{tb}. Then $\tilde{f_r}$ descends to a map f_r on X^{tb}. The image of $\square_k^{tb}$ under f_r is $\square_{k+1}^{tb}$.

Let $q : P_r \to X^{tb}$ be the quotient map identifying the top and bottom edges of the polygon. Let cyl_k be a cylinder, and lift cyl_k to X^{tb}. Call this lift cyl_k^{tb}. Let L and R denote the unidentified left and right edges of the polygon. Inductively define cyl_{k+1} as the closure of $q \circ f_r(\text{cyl}_k^{tb} \setminus (L \cup R))$ with

respect to the linear flow in the $\frac{1}{2-r}$-direction. Observe that cyl_{k+1} doesn't depend on the chosen lift of cyl_k.

Given a geometric armadillo tail with parameter $r = 1/q$, cyl_k lies entirely on $X_{k+1} = \bigcup_{i=1}^{k+1} \square_i$. Then $q \circ f_r(\text{cyl}_k)$ is a subset of a cylinder that lies in $X_{k+1}^{tb} \setminus \square_1$. We will show that there is a circle rotation on $\{0\} \times [0,1]$ that fills in $q \circ f_r(\text{cyl}_k)$ at the points of discontinuity.

We define where the circle rotation is defined, and prove that waist curves of cylinders are periodic points under the circle rotation.

check notation here, and add a few words why this is called a generation zone. We define the *generation zone* as

$$\begin{aligned}\text{generation zone} &= f_r^{-1}(\text{Int}(\text{cyl}_1 \cap \square_2)) \\ &= \left\{(x,y) : \frac{1}{2-r}x < y < \frac{1}{2-r}x + \frac{1-r}{2-r},\ 0 \le x \le 1\right\}.\end{aligned}$$

Given the set of points bsc_k intersects $\{0\} \times [0,1]$ and $\{1\} \times [0,1]$, we remove the points that lie in the generation zone. Why? Under f_r, the generation zone maps into cyl_1. Define sets S_1 (and S_2, resp.) on $\{0\} \times [0,1]$ (and $\{1\} \times [0,1]$, resp.) as the image of the remaining points under f_r. That is,

$$S_1 = \text{proj}_y \circ f_r \left(\gamma \cap \left\{(0,y) : 0 < y < \frac{1}{2-r}\right\}\right)$$

and

$$S_2 = \left\{f_r \left(\gamma \cap \left\{(0,y) : \frac{1-r}{2-r} < y < 1\right\}\right)\right\}$$

where $\text{proj}_y(x,y) = (0,y)$ is the projection onto the y-axis.

We take $q \circ f_r(\text{cyl}_k)$ outside the generation zone and fill it in with a subset of a cylinder, call it cyl'_{k+1}, that lies in $\square_1$. We show that cyl_{k+1} is a union of $q \circ f_r(\text{cyl}_k)$ and cyl'_{k+1}. Let $T : [0,1]/\sim \to [0,1]/\sim$ be a circle rotation where $T(x) = x + \frac{q}{2q-1}$. The map T connect the two sets ($q \circ f_r(\text{cyl}_k)$ and cyl'_{k+1}) at the points of discontinuity.

Figure 5 illustrates the setting.

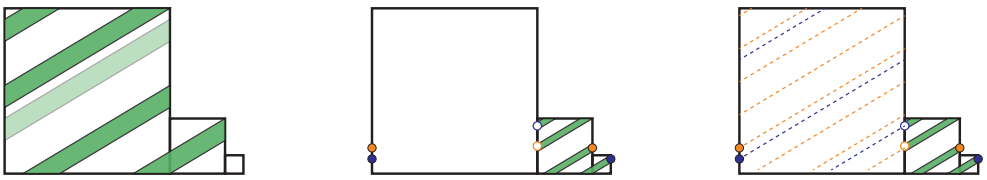

FIGURE 5. $\text{cyl}_1 \setminus$ generation zone(left), $f_r\,(\text{cyl}_1 \setminus \text{generation zone})$ (center), connecting S_1 and S_2 via the circle rotation T (right). The dotted lines represent bsc_2 in $\square_1$.

Theorem 3.3. The circle rotation $T : [0,1]/\sim \to [0,1]/\sim$ where $T(x) = x + \frac{q}{2q-1}$ maps S_1 to S_2 defined above.

In other words, since the circle rotation is a section of the linear flow, we "fill in" $q \circ f_r(\text{cyl}_k)$ at the points of discontinuity to construct cyl_{k+1}.

Remark 3.4. To illustrate the simplest case ($k = 1$) before we prove the general case for all k, take bsc_1, the bottom saddle connection of cyl_1, starting from $(1, 0)$. Bottom saddle connections can be written explicitly, so we consider them instead of waist curves. Since bsc_1 intersects y-axis at

$$\left\{\frac{1}{2q-1}, \ldots, \widehat{\frac{q}{2q-1}}, \ldots, \frac{2q-2}{2q-1}\right\},$$

we have

$$S_1 = \left\{(0, y) : y = \frac{1}{q(2q-1)}, \ldots, \frac{q-1}{q(2q-1)}\right\}, \quad S_2 = \left\{(1, y) : y = \frac{q-1}{q(2q-1)}, \ldots, \frac{2q-2}{q(2q-1)}\right\}.$$

Take $i = 1, \ldots, q-2$, then

$$\frac{i}{q(2q-1)} \xrightarrow{T} \frac{i+q^2}{q(2q-1)} \xrightarrow{T} \frac{i+2q^2}{q(2q-1)} \equiv \frac{i}{q(2q-1)},$$

where $\frac{1}{q} < \frac{i+q^2}{q(2q-1)} < 1$ for $i \in \{1, \ldots, q-2\}$. We note that $\left\{\left(0, \frac{i+q^2}{q(2q-1)}\right)\right\}_{i=1}^{q-2}$ are $q-2$ additional points where we hit the y-axis.

When $i = q-1$,

$$\frac{q-1}{q(2q-1)} \xrightarrow{T} \frac{q-1+q^2}{q(2q-1)} \xrightarrow{T} \frac{q-1+2q^2}{q(2q-1)} \equiv \frac{2q-1}{q(2q-1)}.$$

First note that $\left(1, \frac{2q-1}{q(2q-1)}\right)$ is a singularity. Our claim is that bsc_2' is a saddle connection that is the bottom boundary of cyl_2. Hence take γ to be a waist curve slightly above bsc_2' to avoid the singularity and carry on by iterating T. Also note that $T^{2q-1}\left(\frac{q-1}{q(2q-1)}\right) = \frac{q-1+(2q-1)q^2}{q(2q-1)} \equiv \frac{q-1}{q(2q-1)}$. We will show below that for any $m < 2q-1$, the mth iterate hits the portal of $\square_1$, i.e., $\frac{1}{q} < T^m(\frac{q-1}{q(2q-1)}) = \frac{q-1+mq^2}{q(2q-1)} < 1$. This adds an additional $q-2$ points where we hit the y-axis.

Theorem 3.5. Given a geometric armadillo tail with parameter $r = \frac{1}{q}$ for $q \in \mathbb{N} \setminus \{1\}$, and a cyl_k in the $\frac{1}{2-r}$-direction, cyl_{k+1} exists.

Proof. From the Remark above, we have bsc_2' hitting the y-axis at

$$\left\{\left(0, \frac{i}{q(2q-1)}\right), \left(0, \frac{i+q^2}{q(2q-1)}\right)\right\}_{i=1}^{q-1}.$$

By induction, bsc_k' hits the y-axis at

$$\left\{\left(0, \frac{i}{q^{k-1}(2q-1)}\right), \left(0, \frac{i+q^k}{q^{k-1}(2q-1)}\right)\right\}_{i=1}^{q-1}.$$

Then

$$S_1 = \left\{\left(0, \frac{i}{q^k(2q-1)}\right)\right\}_{i=1}^{q-1}, \quad S_2 = \left\{\left(1, \frac{i+q^k}{q^k(2q-1)}\right)\right\}_{i=1}^{q-1}.$$

Note that $T\left(\frac{i}{q^k(2k-1)}\right) \in S_2$. In other words, the concatenation of $f_r(\text{bsc}_k)$ and bsc_{k+1}' yields the bottom saddle connection of cyl_{k+1}.

This theorem proves that given a cylinder cyl_k on a geometric armadillo tail of parameter $1/q$, we have cyl_{k+1}, which is also a cylinder. □

Corollary 3.6. The skew width of cyl_k in the $\frac{q}{2q-1}$-direction is $\frac{q-1}{q^k(2q-1)}$.

Corollary 3.7. The trajectory starting from $\left(1+\frac{1}{q}+\cdots+\frac{1}{q^{k-1}},0\right)$ in the $\frac{q}{2q-1}$-direction, i.e., bsc_k hits $\{0\}\times[0,1)$ at

$$\begin{aligned}
&\left\{\left\{\frac{1}{2q-1},\cdots,\widehat{\frac{q}{2q-1}},\cdots\frac{2q-2}{2q-1}\right\}+\sum_{i=1}^{k-1}\frac{q-1}{q^i(2q-1)}\right\}\\
\cup\ &\left\{\left\{\frac{i}{q(2q-1)},\frac{i+q^2}{q(2q-1)}\right\}_{i=1}^{q-1}+\sum_{i=2}^{k-1}\frac{q-1}{q^i(2q-1)}\right\}\\
&\vdots\\
\cup\ &\left\{\left\{\frac{i}{q^{j-1}(2q-1)},\frac{i+q^j}{q^{j-1}(2q-1)}\right\}_{i=1}^{q-1}+\sum_{i=j}^{k-1}\frac{q-1}{q^i(2q-1)}\right\}\\
&\vdots\\
\cup\ &\left\{\left\{\frac{i}{q^{k-1}(2q-1)},\frac{i+q^k}{q^{k-1}(2q-1)}\right\}_{i=1}^{q-1}\right.
\end{aligned}$$

where "set + number" indicates that the number is added to every element in the set.

Proof. The proof follows from adding appropriate skew widths to the bottom saddle connections of proceeding cylinders. □

Dami has commented out a bunch of things that might not be necessary. See if what we have here is a sufficient argument.

Figure 6 shows the first few cylinders in this cylinder decomposition for $r=\frac{1}{2}$.

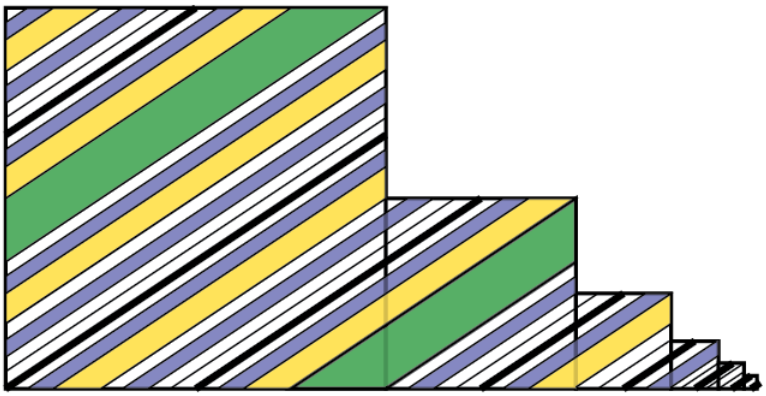

FIGURE 6. Cylinder decomposition on the geometric armadillo tail ($r=1/2$)

Remark 3.8. Given a geometric armadillo tail with parameter $r=\frac{1}{q}$, there exists an infinite cylinder decomposition in the $\frac{1}{2-r}$-direction. The number of times cyl_k intersects the y-axis is $2kq-(2k+1)$. Hence the sum of all skew widths is:

$$\begin{aligned}
\sum_{k=1}^{\infty}(2kq-(2k+1))\cdot\frac{q-1}{q^k(2q-1)} &= \frac{q-1}{2q-1}\sum_{k=1}^{\infty}\left(\frac{2k}{q^{k-1}}-\frac{2k}{q^k}-\frac{1}{q^k}\right)\\
&= \frac{q-1}{2q-1}\left(\frac{2q^2}{(q-1)^2}-\frac{2q}{(q-1)^2}-\frac{1}{q-1}\right)=1
\end{aligned}$$

for all $q\in\mathbb{N}\setminus\{1\}$.

Corollary 3.9. The "actual" width of cyl_k in the $\frac{q}{2q-1}$-direction is $\frac{q-1}{q^k\sqrt{q^2+(2q-1)^2}}$.

4. Area of cylinders

In Corollary 3.9, we found the width of each cylinder. In this section, we will show the length of the waist curve for each cylinder to find the area of cyl_k as a function of q.

First, we will find the horizontal displacement of each waist curve. The table below lists the side lengths of each square and the number of times a waist curve of cyl_k goes through each square. This follows from the circle rotation defined in the previous section.

	$\square_1$	$\square_2$	$\cdots$	$\square_i$	$\cdots$	$\square_k$	$\square_{k+1}$
side length	1	$1/q$		$1/q^{i-1}$		$1/q^{k-1}$	$1/q^k$
#	$k(2q-2)-1$	$(k-1)(q-1)$		$(k-i+1)(q-1)$		$q-1$	1

Then the horizontal displacement of a waist curve of cyl_k is

$$\begin{aligned} & k(2q-2)-1+\frac{1}{q}(k-1)(q-1)+\frac{1}{q^2}(k-2)(q-1)+\cdots+\frac{1}{q^{k-1}}(q-1)+\frac{1}{q^k} \\ = \; & k(2q-2)-1+\sum_{i=1}^{k-1}\frac{(k-i)(q-1)}{q^i}+\frac{1}{q^k} \\ = \; & k(2q-2)-1+\frac{q-1}{q^k}\sum_{i=1}^{k-1}(k-i)q^{k-i}+\frac{1}{q^k} \\ = \; & k(2q-2)-1+\frac{(k-1)q^{k+1}-kq^k+q}{q^k(q-1)}+\frac{1}{q^k}. \end{aligned}$$

For the last equality, we refer to the remark below.

Remark 4.1. The previous computation follows since:

$$\begin{aligned} \sum_{i=1}^{k-i}(k-i)q^{k-i} &= q+2q^2+3q^3+\cdots+(k-1)q^{k-1} \\ &= q+2q^2+3q^3+\cdots+(k-1)q^{k-1}+\left(q+\cdots+q^{k-1}\right)-\left(q+\cdots+q^{k-1}\right) \\ &= 2q+3q^2+\cdots+kq^{k-1}-\frac{q(q^{k-1}-1)}{q-1} \\ &= \left(q^2+\cdots+q^k\right)'-\frac{q^k-q}{q-1} \\ &= \left(\frac{q^2(q^{k-1}-1)}{q-1}\right)'-\frac{q^k-q}{q-1} \\ &= \frac{(k-1)q^{k+1}-kq^k+q}{(q-1)^2}. \end{aligned}$$

Proposition 4.2. The horizontal displacement of the waist curve of cyl_k is

$$(2q-1)\left(k-\frac{q^k-1}{q^k(q-1)}\right)$$

and the actual length of the waist curve, i.e., the circumference of cyl_k is

$$\left(k-\frac{q^k-1}{q^k(q-1)}\right)\sqrt{(2q-1)^2+q^2}.$$

Furthermore, the modulus of cyl_k is given as

$$\frac{\text{circumference}}{\text{width}} = \frac{q^2+(2q-1)^2}{(q-1)^2}\left(kq^{k+1}-(k+1)q^k+1\right),$$

Hooper–Trevnio's inverse modulus and the area of cyl_k is given by

$$\text{area}\,(\text{cyl}_k) = \left(k - \frac{q^k-1}{q^k(q-1)}\right)\frac{q-1}{q^k}.$$

Next, we verify that given $r = 1/q$, the infinite sum of $\text{area}(\text{cyl}_k)$ is equal to $\frac{1}{1-r^2}$, hence there exists an infinite cylinder decomposition in the $\frac{1}{2-r}$-direction.

Proposition 4.3. Given a geometric armadillo tail with parameter $r = \frac{1}{q}$, $q \in \mathbb{N}\setminus\{1\}$, we show that

$$\sum_{k=1}^{\infty}\text{area}\,(\text{cyl}_k) = \frac{1}{1-r^2} = \frac{q^2}{q^2-1},$$

where the cylinders lie in the $\frac{1}{2-r}$-direction.

Proof. We write $\text{area}\,(\text{cyl}_k) = \frac{k(q-1)}{q^k} - \frac{1}{q^k} + \frac{1}{q^{2k}}$. Following the same spirit as a previous remark, we use $\sum\limits_{i=1}^{\infty} ir^i = \frac{r}{(1-r)^2}$, for $|r|<1$. The sum of the first terms is

$$\sum_{k=1}^{\infty}\frac{k(q-1)}{q^k} = \frac{q}{q-1}.$$

The second and third terms are geometric sequences, hence we have

$$\sum_{k=1}^{\infty}\text{area}\,(\text{cyl}_k) = \frac{q}{q-1}+\frac{1}{q-1}+\frac{1}{q^2-1} = \frac{q^2}{q^2-1},$$

our desired result. □

5. No parabolic element

Consider the horizontal cylinder decomposition of the armadillo tail seen in Figure 2. The *perpendicular* cylinder decomposition is comprised of exactly the squares. The element $\begin{bmatrix}1 & 0\\ 1 & 1\end{bmatrix}$ is in the Veech group of the surface and this parabolic element corresponds to the perpendicular cylinder decomposition: indeed, the affine map associated with this Veech group element twists these cylinders, but preserves them as a set.

This phenomenon is understood in the finite translation surface setting, where the existence of a cylinder decomposition with rationally related moduli implies a parabolic element in the Veech group and vice-versa. Here, we see that in the perpendicular cylinder decomposition, the modulus of each cylinder is 1 since each cylinder is a square. However, the moduli of the cylinders in the horizontal cylinder decomposition in Figure 2 goes to infinity, and there is no parabolic element in that direction.

Lemma 5.1. Let $\mathcal{C}$ be a cylinder decomposition on a finite area infinite translation surface. Then if the moduli of the cylinders tend to ∞, there is no parabolic element in the Veech group corresponding to an affine map that preserves the cylinder decomposition.

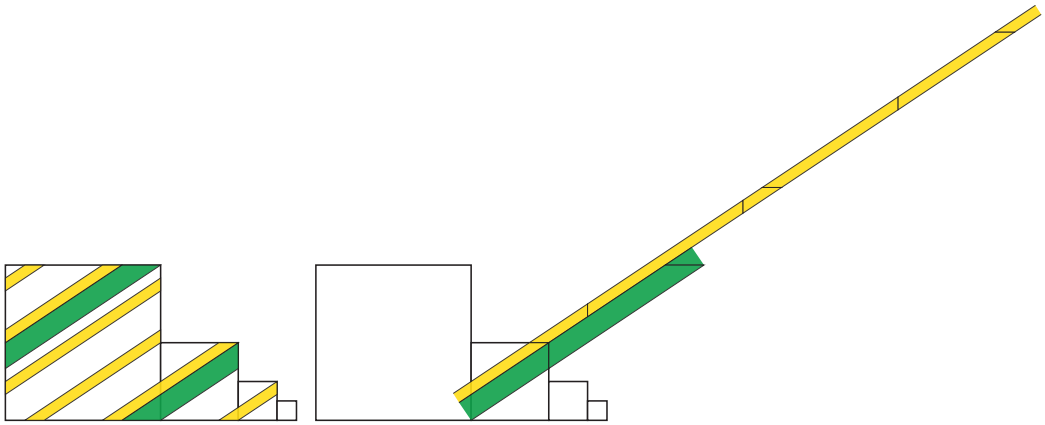

FIGURE 7. Cylinder decomposition $\mathcal{C}$ in the $\frac{1}{2-r}$ direction

Remark 5.2. The lemma allows for rationally related moduli, hence distinguishes the finite translation surface setting from the infinite translation surface setting.

Proof. □

Corollary 5.3. Let $\mathcal{C}$ be the cylinder decomposition constructed in the previous sections of this paper. There is no parabolic element in the Veech group corresponding to this cylinder decomposition.

Proof. We observe that the modulus of cyl_k goes to ∞ as k goes to infinity. □

The following is no longer required! There is no orthogonal decomposition. Write this out carefully.

Lemma 5.4. Let $\mathcal{C}$ be a cylinder decomposition on a finite area infinite translation surface. Then if the moduli of the cylinders tend to 0, there is no parabolic element in the Veech group corresponding to an affine map that preserves the cylinder decomposition.

Proof. □

Merge these two lemmas! Compare to Thurston's construction: when two parabolic elements exist. Then extend it to show when 0 versus 1 versus 2 exist.

Remark 5.5. In work of Hooper and Treviño [7], they observe that the golden ladder has a cylinder decomposition whose moduli are all equal, and the corresponding perpendicular cylinders are symmetric. They are able to find two parabolics, one in each direction. The construction of these parabolics was described by Thurston. .... See the Hooper–Thurston–Veech construction in [4]....

Corollary 5.6. Let $\mathcal{C}$ be the cylinder decomposition constructed in the previous sections of this paper. Then, on $\mathcal{C}^{\perp}$, there is no parabolic element in the Veech group corresponding to this cylinder decomposition.

Proof. We observe that the modulus of $\text{cyl}_k^{\perp}$ goes to 0 as k goes to infinity. From Corollary 3.9 and Proposition 4.2 we have,

$$\begin{aligned}
\text{circumference of } \mathrm{cyl}_k^{\perp} &= \sum_{i=k}^{\infty} \text{width}(\mathrm{cyl}_i) \\
&= \sum_{i=k}^{\infty} \frac{q-1}{q^i\sqrt{q^2+(2q-1)^2}} \\
&= \frac{q-1}{q^k\sqrt{q^2+(2q-1)^2}} \frac{1}{1-1/q} \\
&= \frac{1}{q^{k-1}\sqrt{q^2+(2q-1)^2}},
\end{aligned}$$

$$\begin{aligned}
\text{width of } \mathrm{cyl}_k^{\perp} &= (\text{circumference of } \mathrm{cyl}_k) - (\text{circumference of } \mathrm{cyl}_{k-1}) \\
&= \left(k - \frac{q^k-1}{q^k(q-1)} - \left(k-1-\frac{q^{k-1}-1}{q^{k-1}(q-1)}\right)\right)\sqrt{q^2+(2q-1)^2} \\
&= \frac{q^k(q-1)+1-q}{q^k(q-1)}\sqrt{q^2+(2q-1)^2},
\end{aligned}$$

hence the modulus of $\mathrm{cyl}_k^{\perp}$ is equal to $\dfrac{q(q-1)}{(q^2+(2q-1)^2)\left(q^k(q-1)+1-q\right)}$ □

REFERENCES

[1] Joshua P. Bowman, *The complete family of arnoux–yoccoz surfaces*, Geometriae Dedicata **164** (2012), 113 –130.

[2] ———, *Finiteness conditions on translation surfaces* (Yunping Jiang and Sudeb Mitra, eds.), American Mathematical Society, 2012.

[3] Mirko Degli Esposti, Gianluigi Del Magno, and Marco Lenci, *Escape orbits and ergodicity in infinite step billiards*, Nonlinearity **13** (199907).

[4] Vincent Delecroix, Pascal Hubert, and Ferrán Valdez, *Infinite translation surfaces in the wild*, 2024.

[5] W. Patrick Hooper, *The invariant measures of some infinite interval exchange maps*, Geometry & Topology **19** (2015), no. 4, 1895 –2038.

[6] W. Patrick Hooper, Pascal Hubert, and Barak Weiss, *Dynamics on the infinite staircase*, Discrete and Continuous Dynamical Systems **33** (2013), no. 9, 4341–4347.

[7] W. Patrick Hooper and Rodrigo Treviño, *Indiscriminate covers of infinite translation surfaces are innocent, not devious*, Ergodic Theory and Dynamical Systems **39** (2015), 2071 –2127.

[8] Anja Randecker, *Geometry and topology of wild translation surfaces*, KIT Scientific Publishing, 2016.

[9] Rodrigo Treviño, *On the ergodicity of flat surfaces of finite area*, Geometric and Functional Analysis **24** (2014), 360–386.

[10] Marcelo Viana, *Ergodic theory of interval exchange maps.*, Revista Matemática Complutense **19** (2006), no. 1, 7–100 (eng).